# DESIGN AND FABRICATION OF A COMPOSITE TRANSMISSION HOUSING FOR A HELICOPTOR TAIL ROTOR

ICAS-92-6.7R1

A. F. Johnson and B. Hinz
German Aerospace Establishment (DLR)
Institute for Structures and Design
Stuttgart, Germany

## ABSTRACT

The paper describes a development carried out for Henschel Flugzeug-Werke GmbH for the design and fabrication of a prototype carbon fibre reinforced epoxy (CFRP) transmission housing for the drive gear of a helicoptor tail rotor. Design requirements were for a CFRP housing shell with reduced weight, improved dynamic fatigue strength and better vibration damping compared with a cast aluminium shell. The study shows the feasibility of using carbon fibre fabric reinforcement in a non-axisymmetric shell structure and demonstrates relevant design analysis procedures for the laminated shell structure under complex load conditions.

## 1. INTRODUCTION

This paper describes the development of a prototype CFRP transmission housing for the drive gear of a helicopter tail rotor. The work was carried out in the Demonstration Centre for Composite Materials at the DLR Institute for Structures and Design for Henschel Flugzeug-Werke GmbH, Kassel. Currently the tail rotor gear housing is fabricated as a thin walled cast aluminium shell. The aim of this development project was to examine the feasibility of fabricating the housing from carbon fibre reinforced plastics (CFRP). The main advantages expected from using CFRP are a weight reduction, increased vibration damping, higher strength properties, particularly an improved dynamic fatigue strength.

The closed shell form of the housing is, in principle, very suitable for fabrication in CFRP by filament winding. However, the non-axisymmetric shape requires specially tailored software to drive the filament winding machine, which takes time to produce and can be expensive. There are also problems with the geometrical shape here, in winding fibres with the optimum directions required for the applied loads. It was therefore decided for this demonstration project to use a hand lamination contact-moulding fabrication method, which is well suited to the production of small numbers of components at low cost. The housing was therefore fabricated as two outer flanged CFRP shell halves bonded onto two CFRP cylindrical liners, which were machined to fit the drive unit. Two steel end flanges were bonded between the shell and liners for attachment to the helicopter tail structure. Section 2 contains details of the CFRP laminate construction and the fabrication methods.

In contrast to metals where material properties are fixed, CFRP materials offer the designer a wide range of material properties depending on fibre orientation and laminate construction. It is thus necessary to design a CFRP laminate with the required properties. However, it is not possible to carry out a detailed structural analysis on the housing until the shell wall material properties have been specified. Thus design with composites is an iterative process; first select a laminate structure, then carry out a component analysis and finally refine the material structure to optimize component properties. Details of the materials design and component design calculations are given in Section 3. Using the material properties of the chosen laminate structure a more detailed finite element analysis (FEA) was then carried out to determine maximum deflections, reserve strength factors and to study local loading in the shell wall. These calculations showed that the CFRP housing should have adequate stiffness and strength under short term loads, and that there is scope for further optimisation of the structure.

## 2. FABRICATION OF CFRP HOUSING

### 2.1 Subcomponents of housing

Fig. 1 shows a sketch of the CFRP housing with the three elements of its structure. This consists of:

(a) Two inner CFRP cylindrical liners, which provide a fit for the bearing of the drive unit on each side of the drive.

(b) Two circular steel flanges, bonded to the outside of the CFRP liners and which are used for mounting the housing on the tail structure.

c) Two main CFRP shells, fabricated in two identical halves, bonded together at their common flanges and bonded onto the two flanged CFRP liners.

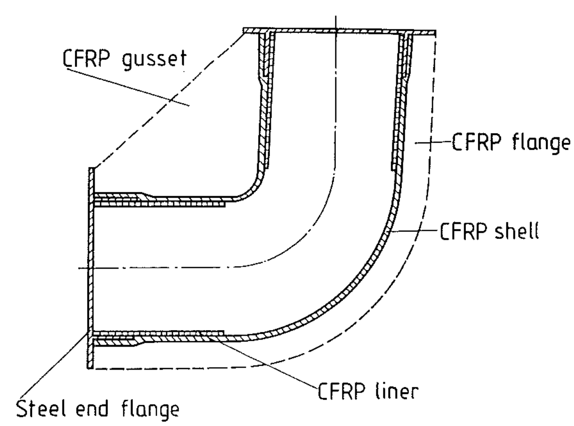


**Fig. 1 CFRP housing construction**

CFRP cylindrical liners

In the structure chosen, the cylindrical liners are not main load bearing. Their purpose is to provide an accurate fit to the drive unit and to transfer loads from the four bearing rings into the shell wall, which is main load bearing. The tubes were filament wound in carbon fibre reinforced epoxy resin, with fibres at $\pm 45°$ to the tube axis, which gives a tube with optimum torsion properties. After cutting to size and machining to a 2mm wall thickness, the cylinders had the steel end flanges shrink fitted and bonded on, see Fig.2.

Laminated CFRP shell

The shell wall is the main loadbearing component in the housing and must carry the loads transmitted from the drive unit through the bearing and liners and the axial load transmitted through the steel flanges. The shell wall is subjected to a combination of bending and torsion loads and as there is no dominant uniaxial load direction, a CFRP laminate with balanced properties is required. This suggests that a CFRP cloth with equal fibres in the warp and weft directions is suitable. In order to provide good flexural and torsional properties in both the straight parts of the housing and in the bend, it is necessary to lay the cloth with alternate plies at 0° and 45° to one of the drive axes. The laminate analysis described in Section 3.2 shows that 12 plies of cloth are required to give the required stiffness and strength properties.

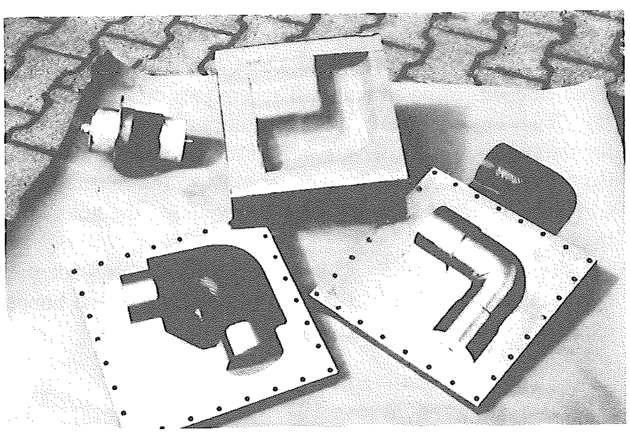

**Fig. 2 Steel form with CFRP components**

A form for the shell wall is shown in Fig. 2 and consists of two steel blocks each machined into a male mould of half the housing and suitable for hand lamination of the two flanged shell halves. A method for applying external pressure during curing of the laminate is required. This was achieved by using the two steel forms to cast the rubber block shown in Fig. 2, which is used to compress the laminate during curing. The rubber block can be made by first coating the steel forms with wax about 3 mm thick or by using an initial hand consolidated shell moulding as a spacer then mounting the forms in a steel box into which a cold curing silicon rubber is poured.

The shell halves were then fabricated by laminating 12 sheets of CFRP cloth on the metal forms, with the warp direction alternatively at 0° and 45° to the drive axis direction, and consolidating each sheet by hand with epoxy resin applied by brush. When consolidated and with a typical fibre volume fraction of 50% achieved by hand laminating, each cloth ply is typically 0.28 mm thick (manufacturers data[1]). Thus the resulting shell laminate should have a wall thickness of 3.4 mm. A high temperature resistant epoxy resin system was chosen suitable for use at the maximum design temperature. The CFRP cloth sheets were cut so that they formed a flange on each side of the shell halves.

After gelation the laminated shells were placed between the steel forms and the rubber block and consolidated by tightening the bolts passing through the steel backing plates. Curing of the laminate took place under pressure and temperature for 15 hours. A completed flanged shell half is shown in Fig. 2.

2.2 Assembly of housing

The housing was assembled by adhesively bonding the subcomponents using a cold curing epoxy resin adhesive. In order to achieve the exact tolerances required for the drive unit, a special assembly jig is required Fig. 3. The adhesive was applied to the cleaned and roughened surfaces of the shell, flanges and liners and the subcomponents placed on the jig where pressure was applied during cure of the adhesive by hand clamps placed across the shell flanges and across the ends of the shell walls. After curing the CFRP flanges were machined to a depth of 20mm. Photographs of the finished housing are shown in Figs. 4. Note that on the inside of the bend the flange was machined to a triangular gusset, thus providing additional stiffening to the structure. The design analysis described in Section 3.3 shows that there is a stress concentration at the centre of the inside flange. Retention of this gusset thus reduces these higher stresses in the structure to a safe level.

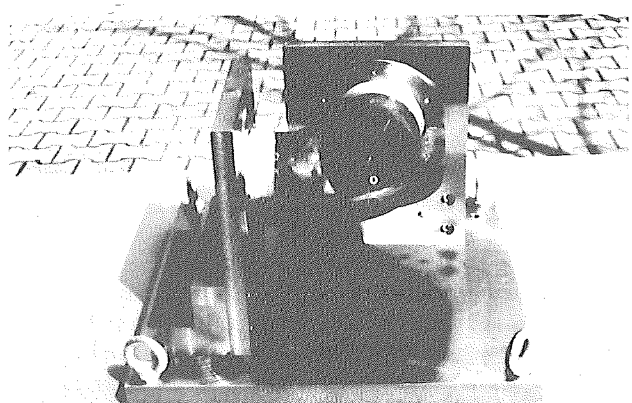

**Fig. 3 Assembly of CFRP housing**

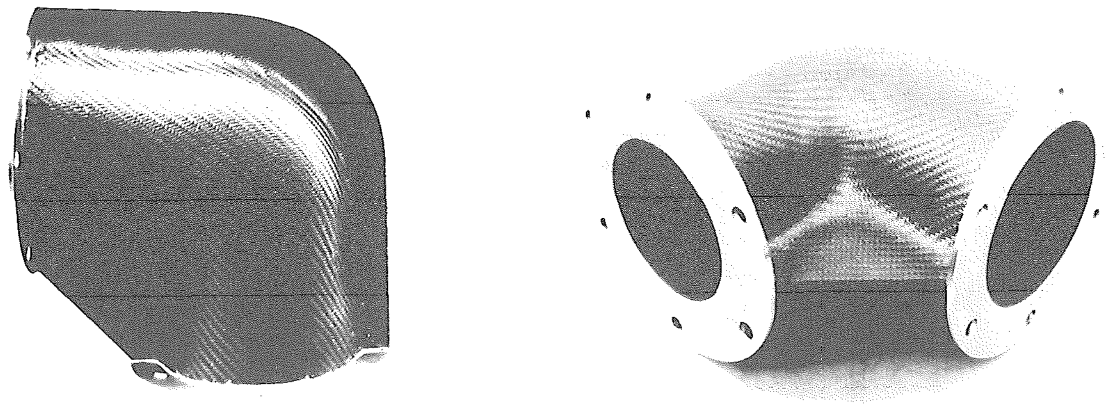

**Fig. 4 The completed CFRP housing**

3. DESIGN CALCULATIONS

Design analysis is required to first determine a suitable laminate structure for the shell wall, and second to establish whether the CFRP housing can withstand the design loads. The materials design calculation is based on a simplified analysis of a cylindrical shell under bending and torsion loads. This is followed by a more detailed FE design analysis to determine the stiffness and strength properties of the CFRP housing under short term static loads for comparison with an equivalent aluminium (Al) housing. In practice temperature cycling, dynamic loads and mechanical fatigue loads are all likely to be important. These factors may need to be taken into account in future analysis, if it is required to optimise the CFRP structure. In the present case the static analysis is used to define safety factors based on typical long term strength properties. If these factors are high enough they should give adequate safety against uncertainties in the dynamic fatigue loads and temperature effects.

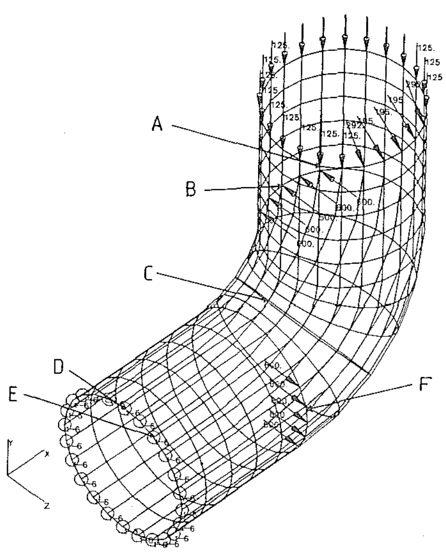


**Fig. 5 FEA model showing loads applied**

3.1 Applied loads

The loads applied to the housing are determined from the drive unit mechanics and are shown in Fig. 5. They consist of transverse (radial) loads on the shell wall applied through the bearing rings, together with axial loads from the drive unit and tail rotor. In the analysis the housing is considered to be clamped at the drive end D in Fig. 5, and loaded by a 3250 N axial load at the free (rotor) end A with 3000 N transverse loads at the internal bearings B, F and a 750 N transverse load at A. Under this load set the housing behaves like a pipe bend clamped at one end under bending and torsion loads.

3.2 Laminate design

The CFRP laminate structure for the shell wall has to be determined initially from a simplified design analysis, since it is not possible to carry out a detailed FE analysis until the laminate structure is known. This initial lay-up can be further refined if necessary after the FE analysis of Section 3.3. The basic structural element of the housing is a cylindrical shell with internal diameter 80 mm subjected to bending and torsion loads. A metal housing in current use would typically be cast aluminium with wall thickness 3 mm. The design criteria therefore used for the CFRP laminate was that it should have similar stiffness properties and improved strength properties to a 3 mm thick aluminium cylinder under the appropriate bending and torsion loads.

As already described in Section 2.1 a balanced weave carbon fibre cloth was chosen for the shell wall, since there is no dominant uniaxial force system in the shell. The cloth with a weight of 245 g/m$^2$ was chosen for its good handling and drape properties on the housing form. When the cloth is oriented along a cylinder giving fibres at 0/90° to the axis the cylinder has good bending but low torsion properties. For optimum torsion properties a cylinder requires fibres at $\pm 45°$ to the axis. Under combined bending and torsion loads a laminate construction was chosen with alternate cloth plies at 0° and 45° to the cylinder axis. The fibre directions in the shell wall are thus 0°, 90°, +45°, -45°, giving a shell with quasi-isotropic properties. This lay-up has the advantage that there is still sufficient fibre reinforcement in the bend of the housing shell, where the cylinder axis rotates through 95°. A laminate analysis is required to calculate the properties of this chosen lay-up and to determine how many plies are required.

| | | Al | CFRP cloth (0°) | CFRP cloth (45°) | CFRP cloth (0°/45°) |
|---|---|---|---|---|---|
| $\rho$ | kg/m$^3$ | 2750 | | 1500 | |
| $E_1=E_2$ | GPa | 70.6 | 55 | 12.2 | 39.2 |
| $G_{12}$ | GPa | 27 | 3.4 | 26.2 | 14.8 |
| $\nu_{12}$ | | 0.3 | 0.05 | 0.8 | 0.32 |
| $\sigma_1 = \sigma_2$ | ST MPa | 300 | 500 | 95.2 | 285 |
| $\sigma_1 = \sigma_2$ | LT MPa | 80 | 300 | 57.1 | 171 |
| $\tau_{12}$ | ST MPa | 100 | 46 | 243 | 135 |
| $\tau_{12}$ | LT MPa | 27 | 28 | 146 | 81 |

**Table 1 Materials data**

Table 1 lists the materials properties used in the laminate calculations and in the subsequent FE analysis. The table shows the densities $\rho$ , the tensile moduli E , shear moduli G , lateral contraction ratios $\nu$ , tensile strengths $\sigma$ and in-plane shear strength $\tau$. The CFRP laminate has orthotropic properties and the subscripts 1 and 2 refer to two orthogonal directions in the laminate. For the basic CFRP cloth data, 1 and 2 refer to the fibre directions. The CFRP data are typical values for a CFRP cloth laminate with 50% fibre volume fraction, based on the suppliers data[1] and previous experience with these materials at the DLR. The data on aluminium refers to alloy WL 3-1854 [2]. The strength data are given as short term (ST) values, and also as long term (LT) values based on design allowable stresses under fatigue loads.

In Table 1 the CFRP (0°) data are the basic ply data for a cloth ply loaded in the fibre directions, i.e. the cloth is oriented at 0° to the laminate 1-axis. The CFRP (45°) data are the properties of the same cloth ply oriented at 45° to the 1-axis, and the CFRP (0°/45°) data refer to a laminate made up of an equal number of 0° and 45° plies. The (45°) and (0°/45°) properties in Table 2 were calculated from the basic (0°) properties using GENLAM [3], a PC based laminate analysis program. The (45°) properties are calculated from the 0° values by rotating the axes. However, for the (0°/45°) laminate the properties may depend on the lay-up details. The calculated values were for a 12 ply symmetric laminate with alternate plies at 0° and 45°; in conventional laminate notation the construction is designated as: $[0/45/0/45/0/45]_s$. Table 1 shows the range of materials properties obtainable in a CFRP cloth laminate, depending on ply orientation and lay-up.

In order to design a laminate with the correct stiffness and strength properties for the housing, we consider a cylindrical element of the housing, consisting of the flanged cylinder shown in Fig. 6. From the loads applied to the housing, it is possible to calculate the maximum bending and torsion moments acting on a cylindrical cross-section. With the (x,y,z) axes as shown in Fig. 6 and assuming that the housing bend lies in the (x,y) plane, these are:

| | |
|---|---|
| In-plane bending moment: | $M_z$ = 327 Nm |
| Out-of-plane bending moment: | $M_y$ = 103 Nm |
| Torsion moment: | $M_x$ = 70 N |

Here the subscripts x, y, z refer to the axis about which bending or torsion take place, and "in-plane" refers to bending in the (x,y) plane of the housing bend. Thus we see that the highest bending moment is in-plane due to the rotor axial force.

The required properties of the flanged cylinder element unter these loads are the flexural rigidities about the y- and z-axes, the torsional rigidity T, and the corresponding bending and twisting moments at failure M*.These properties can be calculated in terms of the cylinder wall thickness and flange geometry using standard design formula for beams and cylinders, see for example Young [4], with the materials property data from Table 1. Table 2 shows the results of such calculations for an Al cylinder, without a flange, and for the CFRP cylinder with flange. The cylinder element is assumed to have an internal diameter of 80 mm, and for Al a wall thickness of 3 mm. After trial calculations with different laminate lay-ups a CFRP cloth laminate with 12 plies and a symmetric construction $[0,45,0,45,0,45]_s$ was chosen. As discussed in Section 2.1, such a laminate has a design thickness of 3.4 mm. The flange geometry assumed in the calculations is a depth of 20 mm and a thickness of 6.8 mm (i.e. 2x3.4 mm). All the strength calculations were based on the long term (LT) design allowable stresses given in Table 1.

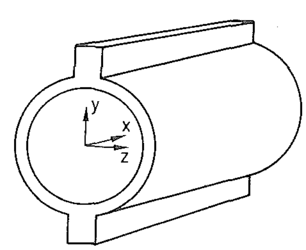


**Fig. 6 Flanged cylinder element**

| | | | 3 mm Al | 3.4 mm CFRP | 3.4 mm CFRP +2 mm liner |
|---|---|---|---|---|---|
| Flexural rigidity | kNm² | $D_z$ | 47.6 | 56.7 | 62.4 |
| | | $D_y$ | 47.6 | 30.4 | 36.1 |
| Torsional rigidity | kNm² | T | 36.7 | 23.0 | 47.9 |
| Flexural strength | Nm | $M_z$* | 1255 | 4360 | >4360 |
| | | $M_y$* | 1255 | 3164 | >3164 |
| Torsional strength | Nm | $M_x$* | 840 | 2646 | >2646 |

**Table 2 Calculated properties of flanged cylinder element**

Table 2 shows that the chosen CFRP laminate structure has similar stiffness properties and improved strength properties compared with the Al cylinder. In particular the in-plane flexural rigidity $D_z$ of the CFRP cylinder is higher than that of the Al cylinder, whilst the transverse flexural rigidity $D_y$ and torsional rigidity T are lower. The flexural and torsional strength properties of the CFRP cylinder are predicted to be about three times higher than those of the Al cylinder and well above the applied bending and torsion moments. It was shown above that the maximum applied inplane bending moment $M_z$ is about three times higher than the transverse bending moment $M_x$, thus the lower transverse flexural rigidity $D_y$ is not expected to be a problem as it is in the direction of lowest bending load.

Table 2 also shows calculated properties for the CFRP shell with the 2 mm CFRP liner. The liner was filament wound at ±45° fibre angle in order to improve its torsional properties. The materials data in Table 1 for the (+45°) CFRP cloth will be similar to the properties of the liner. Using the data the additional stiffness in the cylinder wall could be calculated due to the liner. The table shows that the combined torsional rigidity is now higher than that of the Al cylinder. Since the maximum twisting moments $M_x$ are expected to be in the clamped cylindrical end of the housing, where the liner is present, the housing is expected to have sufficient torsional stiffness.

One further check made on the CFRP shell laminate construction was to calculate the combined effect of the bending and torsion loads on the laminate strength, since the shell wall is in a state of multiaxial stress - biaxial tension/compression combined with in-plane shear. From the maximum bending and torsion loads given above the shell wall in-plane loads can be calculated: $N_1$, $N_2$ in the axial and circumferential directions, and $N_{12}$ the in-plane shear load. In the worst case when all loads reach a maximum at a single point in the cylinder wall (not likely to happen), the combined loading at that point is

$$N_1 = 64 \text{ N/mm}, N_2 = 20 \text{ N/mm}, N_{12} = 7 \text{ N/mm}.$$

On using the laminate program GENLAM [3] for the 12 ply CFRP cloth laminate, with this combined load system and using a quadratic composite material failure criterion, a reserve strength factor R can be calculated. It was found that R = 12.6, where R > 1 indicates a factor of safety. This factor is high showing that there is adequate reserve strength in the shell wall, and suggests that there is scope for optimisation of the laminate structure by a reduction in the number of plies.

### 3.3 FEA of housing

The calculations described above were used to select a suitable CFRP laminate construction for the housing. In this section a more detailed FE design analysis is carried out with the chosen laminate to examine the influence of housing geometry, loads and fixing conditions. In the absence of specific design criteria for the housing the FE analysis compares the behavior under load of the CFRP housing with that of an Al housing. The FE analysis is also based on a geometrical model of the housing in which certain simplifying assumptions are made, for example that the angle between the two axes is 90° instead of 95°. However, the model has the main features of the housing geometry, and can be refined further later if necessary.

#### FEA model

Fig. 5 shows the housing geometry with the applied loads as used in the FEA model. The two cylindrical sections have diameter 80 mm (between the shell middle surfaces) and lengths 85 mm at the drive end and 80 mm at the rotor end. These cylinders are connected by an elbow section with interior angle 90°. Details of the applied loads and edge conditions were discussed in Section 3.1. In the FE model at the drive end D all node displacements and rotations were suppressed whilst the rotor end A was unconstrained. The loads at the internal bearings were applied over 60° arcs in the shell wall. The FEA was carried out at the DLR using the pre- and postprocessor PATRAN [5] with the FE software PERMAS [6] on an Apollo 3500 workstation.

The Al housing was modelled by 360 4 node QUAD 4 isotropic thick shell elements which contain bending, membrane and through-thickness shear stresses. The elements were all 3 mm thick and the Al materials data from Table 1 was used. The steel flange at the rotor end was modelled by superimposing on the shell 36 BAR 2 beam elements, which

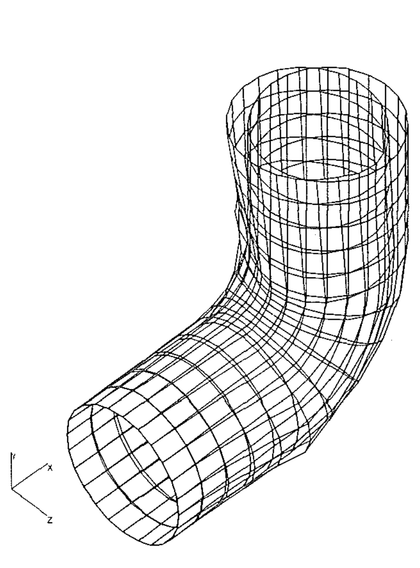

**Fig. 7** **FEA results - housing deformation under load**

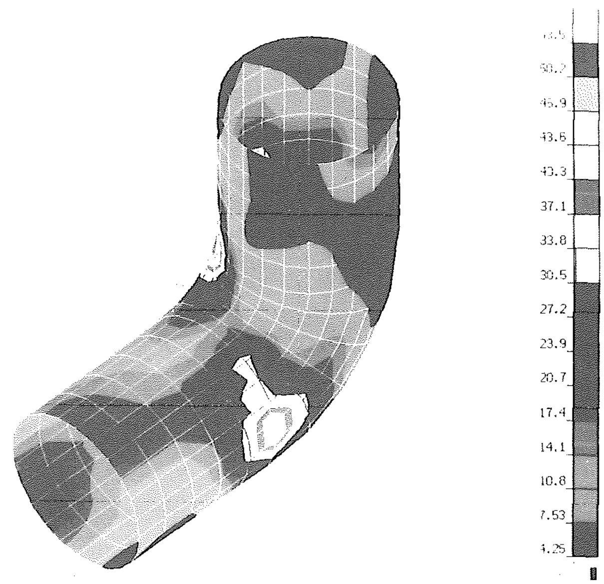


**Fig. 8** **FEA results - housing stresses**

support tensile and bending loads. The beam elements were assigned the properties of a steel flange with cross-section 10 mm x 3 mm. Thus the loads there were applied to the shell stiffened by a steel flange. Because the edge at D was assumed to be clamped, it was not necessary to include a similar steel flange at this edge in the model.

The CFRP housing was modelled by 360 4 node QUAD 4 anisotropic thick shell elements. The elements were 3.4 mm thick and the materials data for the (0°/45°) CFRP material in Table 1 were used, with the (1,2) material axes chosen to be parallel to the rectangular element axes. The contribution from the CFRP liners to the housing stiffness properties was not included in the model, although this refinement could be added if required. The thick shell element models through thickness shear effects in the shell wall, which can be important in composite laminates. An estimated value for the through thickness shear modulus $G_{13}$ = 10 GPa was used in the calculations. The CFRP housing had the same steel flange elements as the Al housing. The two CFRP flanges were modelled by a further set of 60 BAR 2 beam elements superimposed on the shell elements. These flanges had a cross-section geometry of 20 mm x 6.8 mm and were assigned the same material properties as the shell wall. Note that the beam elements appear as lines on Fig. 5 and hence cannot be distinguished in the figure from the lines connecting the nodes.

FEA results

Fig. 7 shows the computed CFRP housing deflections under the load system. Note that the actual deflections are magnified in the figures so that the modes of deformation can be easily seen. The deformation of the housing is seen to be a complex mixture of compression in the y-direction due to the axial force, bending about the z-axis at the bend of the elbow, transverse bending about the y-axis, torsion about the x-axis, and local shell deformations due to the concentrated line loads applied. The main deformations are in the y-z plane due to the axial thrust and radial loads. Table 3 gives computed deflection components $u_x$, $u_y$, $u_z$ at the points A and B , see Fig. 5, for the CFRP and Al housings. The point B is the position of greatest deflection in the shell, and point A also has a large displacement. At all other points in the shell the deflections are less than those computed at point B. Table 3 shows that the CFRP shell has a maximum deflection about 25% higher than the Al shell under the same load system. However the maximum deflection of 0.31 mm due mainly to the radial thrust at A is still very small.

The stress field in the CFRP housing is shown in Fig. 8 as contours of the quadratic equivalent stress function $\sigma = ( \sigma_{11}^2 + \sigma_{22}^2 - \sigma_{11}\sigma_{22} + 3\sigma_{12}^2 )^{1/2}$ . This function represents the von Mises equivalent stress function in a metal and for a CFRP laminate with quasi-isotropic properties it is numerically close to the stress function used in the Tsai-Wu failure criterion. Fig. 8 shows clearly the high stress regions in the bend of the housing, under the line loads at B and F and at the clamped end. Away from these local high stress regions equivalent stresses are low, typically < 10 MPa. Study of the computed stress values shows that the highest stresses are at B due to the radial line load. Table 3 lists computed in-plane stresses at these critical points for the CFRP and Al housings. The notation for the stresses here is that 1 and 2 refer to the local element axes, with the 1-axis aligned longitudinal to the cylinder wall, and the 2-axis transverse to it. The highest stress in the housing is at point B under the local bending of the shell wall due to the radial load. Point E has a raised stress level due to the end clamping. Table 3 shows that the maximum shell wall stresses in the Al housing are higher than in the CFRP housing, typically 25% higher at point B, but up to 100% higher at the clamped end E. A study of the contour plots of stress for the Al housing (not shown here) indicates that average stresses are typically 25% higher than in the CFRP housing. On comparing the maximum tensile and shear stresses with the long term (LT) material strength properties

| Position (Fig. 5) | CFRP | | | Al | | |
|---|---|---|---|---|---|---|
| Displacement:mm | $u_x$ | $u_y$ | $u_z$ | $u_x$ | $u_y$ | $u_z$ |
| A | -0.074 | -0.17 | -0.21 | -0.089 | -0.11 | -0.20 |
| B | -0.015 | -0.15 | -0.31 | -0.02 | -0.12 | -0.24 |
| Stresses MPa | $\sigma_{11}$ | $\sigma_{22}$ | $\sigma_{12}$ | $\sigma_{11}$ | $\sigma_{22}$ | $\sigma_{12}$ |
| Wall: | | | | | | |
| B | 65.1 | 30.6 | 16.5 | 78.5 | 39.0 | 22.4 |
| E | 23.3 | 4.3 | 6.6 | 48.4 | 8.4 | 1.6 |
| Flange: | | | | | | |
| C | 14.6 | 6.5 | 8.1 | - | - | - |
| D | 31.5 | 6.4 | 2.1 | - | - | - |
| Reserve Strength Factors | $R_1$ | $R_2$ | | $R_1$ | $R_2$ | |
| B | 4.6 | 4.9 | | 1.0 | 1.2 | |
| E | 12.9 | 12.3 | | 1.7 | 16.8 | |

**Table 3 Computed maximum deflections and stresses**

in Table 2, we can calculate reserve strength factors

$$R_1 = \sigma_1/\sigma_{11}, \ R_2 = \tau_{12}/\sigma_{12}$$

These are also given in Table 3 for the stresses at points B,E and show that the CFRP housing has much higher reserve strength factors, $R_1$ = 4.6, 12.9, $R_2$ = 4.9, 12.3, compared with the Al housing $R_1$ = 1.0, 1.7, $R_2$ =1.2, 16.8. The CFRP factors are high and suggest that the housing has adequate reserve strength. The factors for the Al housing are low and indicate that under dynamic fatigue conditions failure may occur under local loads.

One reason for the lower stresses in the CFRP housing, is that loads are also taken by the CFRP flanges. The FE analysis computes the bending and torsion moments in the flange elements. The maximum values are found to be at the intersection of the CFRP flange with the clamped end, point D, and at the inside of the bend, point C. From these maximum moments it is possible to calculate the maximum stresses in the flanges, and these are shown in Table 3. The highest stress is seen to be 31.5 MPa at the clamped end. Although this is higher than the average wall stress (≅ 10 MPa ), it is less than the maximum stress in the wall at point B. Note that this high flange stress occurs at the point where the housing is strengthened by the steel end flange. The maximum stress at the flange bend, point C, is not particularly high, suggesting that the large triangular gusset, added there in the fabricated component (see Fig. 4) could be reduced in size.

## 4. CONCLUSIONS

1. The study demonstrates the feasibility of fabricating a non-axisymmetric transmission housing from two compression moulded CFRP shells bonded to cylindrical liners at a common flange.
2. Based on a simplified analysis of a flanged cylinder element under bending and torsion loads, a laminate construction of 12 plies of CFRP fabric with a quasi-isotropic lay-up was determined.
3. Detailed FEA showed that shell wall stresses are low, typically 10-15 MPa, except at stress concentrations due to local radial loads from the drive bearing.
4. At these stress concentrations strength reserve factors are greater than 4.6 for the CFRP housing compared with values of about 1 for the Al housing, showing that the CFRP housing has adequate reserve strength.
5. Deflections in the CFRP housing are about 25% higher than an Al housing, however the maximum predicted deflection of 0.31 mm is still low.
6. The analysis suggests there is further scope for optimising the CFRP construction through a reduction in wall thickness or flange geometry.

## ACKNOWLEDGEMENTS

The authors wish to acknowledge Henschel Flugzeug-Werke GmbH for supporting the project, for valuable discussions and for providing the steel forms. They also thank their colleagues B Heidenreich and U Reifegerste for their help in the fabrication of the prototype.

## REFERENCES

1. INTERGLAS AG Technische Datenblätter Nr. 303/89, 1989.
2. Werkstoff-Handbuch der Deutschen Luftfahrt I/2Leichtmetalle, DK 669.7 : 629.73 WL 3.1854 Beuth Verlag, 1986.
3. GENLAM, Think Composites, P.O.Box 581, Dayton,Ohio, 1988.
4. W.C.Young: Roark's Formulas for Stress and Strain, 6th edition, McGraw-Hill, 1989.
5. PATRAN 2.3, PDA Engineering, 2975 Redhill Avenue,Costa Mesa, California, 1988.
6. PERMAS, 3.04C, INTES, Nobelstr. 15, D-7000 Stuttgart 80, 1990.